Nadimi, S. & Fonseca, J. *Géotechnique* [http://dx.doi.org/10.1680/jgeot.15.T.033]

TECHNICAL NOTE

Enhancing soil sample preparation by thermal cycling

S. NADIMI* and J. FONSECA*

The fabrication of soil samples of uniform density is a fundamental problem in laboratory and physical experiments. A novel technique that relies on a systematic increase of density induced by thermal cycling is presented here. The principle is simple; when the sample is heated the grains and their container undergo thermal expansion and this leads to the settling of the material due to the differential thermal expansion between the grains and the container and the metastable nature of the granular assembly. This change in fabric is not reversible upon cooling down of the sample, so the newly formed fabric can be used for experimental testing. Moreover, the soil fabric can be incrementally enhanced using successive thermal cycles of heating–cooling. In this paper, the change of void ratio is investigated in two carbonate sands, a silica sand and glass ballotini. The effect of particle morphology and initial density on the thermal-induced mechanisms of grain rearrangement is discussed. On the basis of experimental results we hypothesise that thermal cycling enables laboratory samples to be produced with enhanced densities and better soil–boundary interfaces, which is critical to help interpretation of data in experimental and numerical tests.

KEYWORDS: fabric/structure of soils; sands; temperature effects

INTRODUCTION

For the most part, the behaviour of soil has been investigated using laboratory-prepared samples. Depending on the mode of deposition and the grain morphology, different topological configurations in terms of grain rearrangements and void geometries may emerge, and this has a fundamental role in determining the properties of the material being measured (Butterfield & Andrawes, 1970; Miura & Toki, 1982; Rad & Tumay, 1987; Fonseca *et al*., 2013). While the uniformity of the sample is a matter of concern, there is limited control on the local void ratio variations and the contact topologies obtained using either gravity-induced deposition or mechanical-energy-based methods.

For samples produced by different air pluviation configurations, the density within the granular medium appears to be non-uniform (Vaid & Negussey, 1984). In fact, higher densities are often attained in the central part of the sample and lower densities at the boundaries (e.g. Camenen *et al*., 2013). Marketos & Bolton (2010) have pointed out that not only the lower void ratio attained at the boundary of the sample, but also the low number of contacts in the soil–boundary interface affects the soil behaviour measured from laboratory testing.

A key aspect in sample preparation is to mimic in situ characteristics such as relative density and soil fabric as closely as possible. Intact sand, in particular older formations, possess mature fabrics that have developed during geological history, which can hardly be reproduced using conventional laboratory techniques. Cuccovillo & Coop (1997) have shown that the low void ratio values found for intact samples of Greensand could not be attained in the laboratory by loading the sample to values closer to the overburden stresses experienced by the intact material. Fonseca *et al*. (2012) used a combination of pouring and tamping to prepare reconstituted samples with densities close to the intact values. However, these mechanical processes have led to the disintegration of pre-cracked grains and, thus, have produced samples with distinct fabric, grading and contact topologies and consequently a distinct mechanical response when compared to the intact sand.

Increasing computation power has enabled numerical simulations to model the discrete nature of soil, and validation of the numerical results requires better and more controllable physical samples. Difficulties in obtaining the same void ratio values for laboratory samples and discrete-element method specimens obtained using an analogous process have been highlighted previously (e.g. O'Donovan *et al*., 2015). It is clear from previous studies that the laboratory characterisation of soil response requires enhanced sample fabrication able to provide more uniform specimens with more stable and controllable fabric, and these are the key aspects that the technique presented here is intended to advance.

EXPERIMENTAL METHOD

The technique presented here consists of making use of thermal energy to enhance the granular packing of sand for laboratory testing. This work draws upon previous studies on the dynamics induced by thermal cycling on granular media (Chen *et al*., 2006; Percier *et al*., 2013). The rise in temperature results in a thermal expansion of the grains and the container, which causes the granular assembly to settle and densify. The change in the density of the sample is a function of the differential thermal expansion between the grains and the container. Bringing the sample back to room temperature does not alter the newly formed fabric, so the sample can be used for laboratory and physical testing. The packing of the grains can incrementally be enhanced using successive thermal cycles of heating–cooling; termed thermal cycling herein. Figure 1 shows a schematic diagram of how thermal cycling acts in producing a more compacted fabric.

Manuscript received 29 September 2015; revised manuscript accepted 25 April 2016.
Discussion on this paper is welcomed by the editor.
* Department of Civil Engineering, City University London, London, UK.

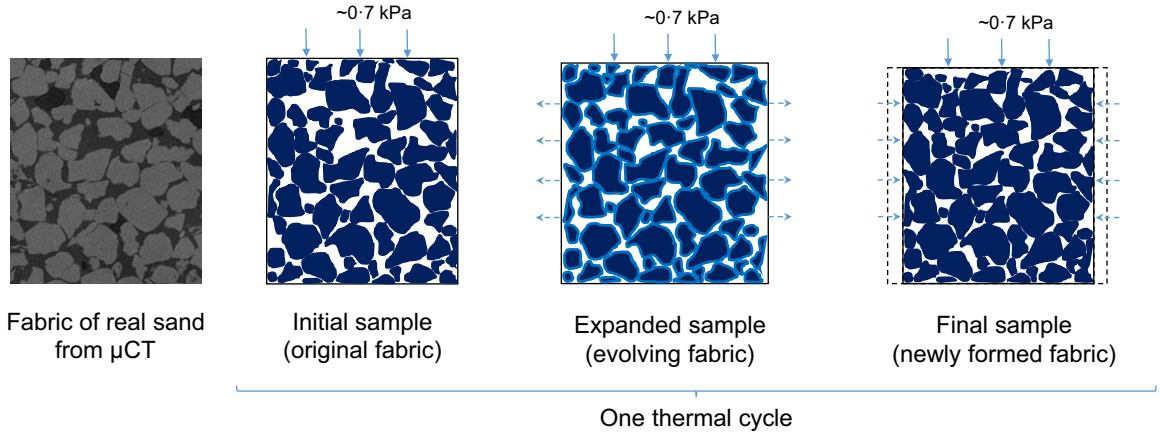

Fig. 1. Schematic diagram illustrating the evolution of the internal fabric of a natural sand under thermal cycling; initial fabric taken from a tomography image (μCT)

Table 1. Physical properties of granular materials used

	d_{50}: μm	G_s	e_{min}	e_{max}	C_u (d_{60}/d_{10})
Fine carbonate sand	240	2·71	0·98	1·87	2
Coarse carbonate sand	570	2·82	0·83	2·38	2·8
Silica sand	840	2·65	0·51	1·01	1·5
Glass ballotini	180	2·50	0·50	0·75	1·1

Materials

The materials used in the experiments were: a fine graded Dogs Bay carbonate sand from the Republic of Ireland (Klotz & Coop, 2001); a coarse graded carbonate sand from the Persian Gulf (Fonseca *et al.*, 2015); a silica Leighton Buzzard sand; and glass ballotini. The material properties are presented in Table 1 and the particle size distributions (PSDs) of all four materials are shown in Fig. 2. The sands had been chosen for their diverse properties, that is, mineralogy and particle morphology, and their extensive use in previous research. The carbonate sands are made from the remains of marine organisms, such as shells and skeletal materials. These shelly grains are angular and tend to form loose fabrics. Moreover, the relative softness of the grains makes them more susceptible to crushing under relatively small loads. Leighton Buzzard sand is part of the Lower Greensand formation from the UK; it comprises angular to sub-angular particles, free of silt or clay (Klotz & Coop, 2001).

Cylindrical containers made of poly(methyl methacrylate) (PMMA) and aluminium, with the dimensions as specified in Fig. 3, were used. This is believed to be representative of the vessels commonly found in soil mechanics laboratories.

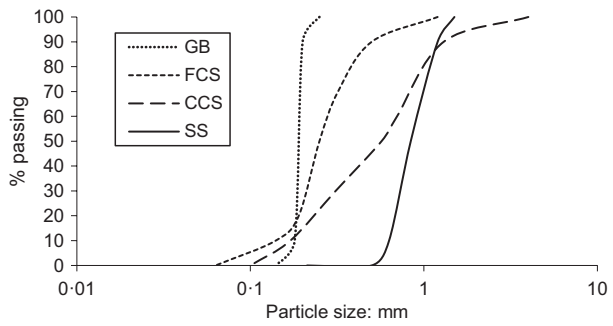

Fig. 2. Particle size distributions for the four materials: glass ballotini (GB), fine carbonate sand (FCS), coarse carbonate sand (CCS) and silica sand (SS)

Sample preparation and void ratio measurements

The samples were prepared using the air pluviation method as described by Cavarretta (2009). This technique consists of filling the throat of the funnel at each deposition step while keeping it in contact with the top surface of the soil. The throat is then raised and the soil is deposited without excessive impact or agitation. Tapping on the sides of the container was applied to produce the denser samples and a slight tapping was also used at the end of the pluviation process in order to create a flat surface; this is particularly important for the accuracy of the void ratio measurements. A height over diameter ratio (H/D) of approximately 1·2 was used for all samples.

For the measurement of the global void ratio, the height of the sample was obtained by averaging four equally spaced reading points on the sample's top surface using a depth gauge (precision of 0·01 mm) and the mass of soil was measured with a precision of 0·01 g. The specific gravity values provided in Table 1 were used.

Experimental set-up

A piston was placed on top of the sample and a small dead weight of approximately 0·7 kPa was applied; a schematic diagram of the set-up is shown in Fig. 3. The temperature was increased from a room temperature of approximately 25 to 85°C, in other words, $\Delta T = 60$°C. The sample was kept in the oven for 9 h to ensure that the same temperature was reached throughout the granular system. Subsequently, the sample was cooled down to the initial room temperature and the void ratio measurements were taken after 15 h. Each cycle took 24 h. In total, 15 tests were carried out, of which nine were stopped after five cycles and only six were stopped after 20 thermal cycles (Table 2).

RESULTS AND DISCUSSION

The void ratio values at the end of each cycle were measured in terms of the change in height of the sample or

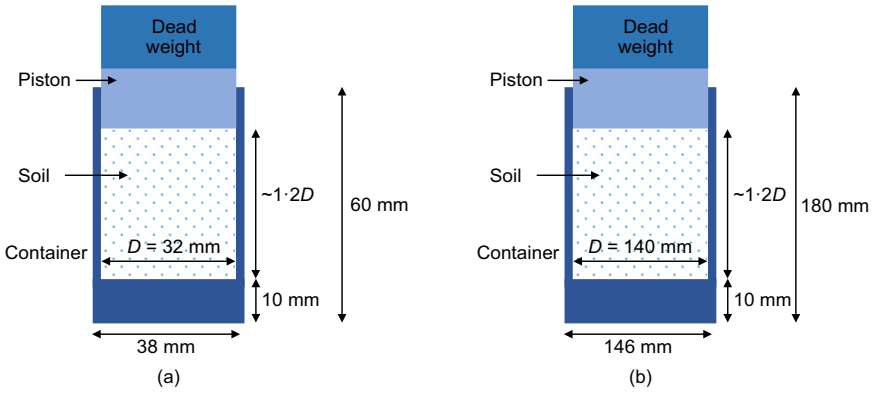

Fig. 3. Schematic diagram of set-up used in experiments, including details of sample and container sizes (*H* being the initial height of the sample and *D* the internal diameter of the container): (a) PMMA container; (b) aluminium container

Table 2. Summary of results obtained from thermal cycling experiments

Test ID*	*H*	*H*/*D*	Cycle number	e_i	e_f	Δe	D_{r_i}: %	D_{r_f}: %	ΔD_r: %
GB-P32a	37·86	1·18	5	0·642	0·631	0·011	43·2	47·6	4·4
GB-P32b	36·60	1·14	20	0·605	0·570	0·035	58·0	72·0	14·0
			5		0·594	0·011		62·4	4·4
SS-P32a	39·00	1·22	20	0·699	0·574	0·125	62·2	87·2	25·0
			5		0·627	0·072		76·6	14·4
SS-P32b	38·28	1·20	5	0·658	0·626	0·032	70·4	76·8	6·4
SS-P32c	37·78	1·18	5	0·621	0·599	0·022	77·8	82·2	4·4
FCS-P32a	41·90	1·31	5	1·465	1·394	0·071	45·5	53·5	8·0
FCS-P32b	39·98	1·25	20	1·395	1·279	0·116	53·4	66·4	13·0
			5		1·333	0·062		60·3	6·9
FCS-P32c	39·72	1·24	5	1·320	1·273	0·047	61·8	67·1	5·3
CCS-P32a	40·47	1·26	5	1·533	1·430	0·103	29·7	40·0	10·3
CCS-P32b	41·18	1·29	5	1·377	1·322	0·055	45·3	50·8	5·5
CCS-P32c	39·91	1·25	5	1·165	1·111	0·054	66·5	71·9	5·4
GB-P140	142·58	1·02	5	0·623	0·610	0·013	50·8	56·0	5·2
GB-A140	176·95	1·26	20	0·732	0·699	0·033	7·2	20·4	13·2
SS-A140	177·19	1·27	20	0·717	0·696	0·021	58·6	62·8	4·2
FCS-A140	177·40	1·27	20	1·467	1·449	0·018	45·3	47·3	2·0

*Test ID includes granular material abbreviation (GB, glass ballotini; SS, silica sand; FCS, fine carbonate sand; CCS, coarse carbonate sand), material of container (P, PMMA; A, aluminium) and container's internal diameter.

settlement of the piston. The top surface of the sample was found to be fairly levelled after thermal cycling, which is in part related to the effect of the dead weight, but also suggests that packing densification is a bulk effect rather than a boundary effect; this has also been observed by Chen *et al.* (2006). The densification was assessed in terms of relative density, $D_r = (e_{max} - e)/(e_{max} - e_{min}) \times 100$.

Effect of container and initial density

The most significant change in density was obtained using a PMMA container; that is, ΔD_r values of 25% for the silica sand and 13% for the fine carbonate sand were measured at the end of 20 thermal cycles, compared with much lower values of 4·2 and 2% for the aluminium container. The incremental changes throughout the 20 thermal cycles are presented in Fig. 4(a) for the silica sand and Fig. 4(b) for the fine carbonate sand. For both sands the PMMA container exhibits, clearly, a more marked relaxation.

The experiments carried out on glass ballotini also confirmed a significant densification using the PMMA container, with a final void ratio of 0·57 (very close to e_{min}) attained at the end of 20 cycles (Fig. 5(a)). In this case, however, the ΔD_r values measured for the PMMA and aluminium containers were similar, namely, 14 and 13·2%, respectively. This can be related to the distinct initial void ratio of the two samples; thus, the results were plotted using a normalised void ratio, which again shows better results using the PMMA container (Fig. 5(b)).

The greater densification obtained using a PMMA container can, in part, be explained based on the expected linear expansion of the grains and the container presented in Table 3, for a ΔT of 60°C. A linear expansion of 0·46% of the total diameter is expected for the PMMA container and only 0·14% for the aluminium container, therefore explaining the lower efficiency of the latter. The expected expansion of the grains is lower for the carbonate sand (0·04% of the mean diameter) and larger for the silica (0·10%), with the glass ballotini in between (0·05%). Since the *H*/*D* ratio of the sample is kept constant, the effect of increasing the sample diameter on the diametrical expansion is compensated by the reduction of the height so the overall volumetric or bulk expansion is not expected to be affected.

Effect of grain morphology and packing

As shown in Fig. 4 and Fig. 5, when subjected to multiple successive thermal cycles, the density of the granular system continues to increase, while the increment after each cycle

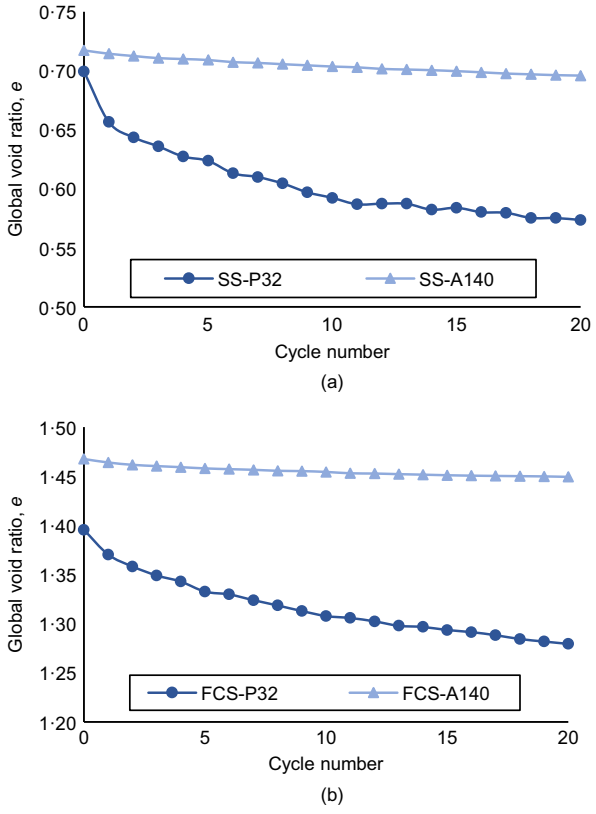

Fig. 4. Void ratio evolution for 20 thermal cycles for: (a) silica sand (SS); (b) fine carbonate sand (FCS), for a PMMA container (P32) and an aluminium container (A140)

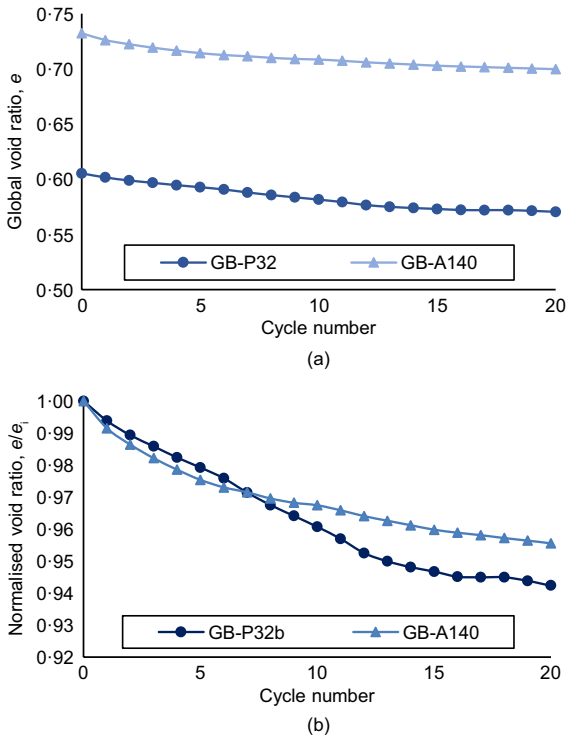

Fig. 5. Void ratio evolution for 20 cycles of a sample of glass ballotini (GB) for a PMMA container (P32) and an aluminium container (A140): (a) using the global void ratio; (b) using the global void ratio normalised by the initial void ratio

tends to become progressively smaller. In fact, after five thermal cycles and for the PMMA container, the void ratio reduction measured for the silica and the fine carbonate sands was more than 50% of the value attained at the end of 20 cycles and after ten cycles the values were as high as 86 and 75%, respectively. The Δe values measured for the glass ballotini were much lower compared with the sands and the reduction was seen to be more gradual throughout the 20 cycles. The lower susceptibility of the glass ballotini to compact under thermal cycling can be attributed to the limited packing configurations that mono-sized spheres exhibit and the more stable fabric when compared with the packing of irregular shaped sand grains.

The ability of thermal cycling to densify samples of the three sands with different initial densities is demonstrated in Fig. 6(a) for the coarse carbonate, Fig. 6(b) for silica sand and Fig. 6(c) for the fine carbonate sand. In addition, when comparing the change in relative density for each specimen, as presented in Table 4, it can be seen that greater values were measured for the samples with lower initial density, with particularly high values for the silica sand.

Although for the two carbonate sands the final relative densities attained were lower than the silica sand, the results are very satisfactory given the difficulties in obtaining D_r values greater than 60% without breakage of the grains. In fact, Wils *et al.* (2013) report on the limitations of using standard densification techniques, such as described in ASTM (2016) for carbonate sands, and they cause grain crushing which alters the e_{min} value and the upper limit of D_r.

Thermally induced grain rearrangement

Granular systems form contact networks of stress-transmitting grains able to resist external loads and other mechanical perturbations, and this increases the resilience of the material to changes in fabric under static loading (Fig. 7(a)). It is suggested here that the small disturbance induced by thermal variations causes breakage of force chains, as discussed in Cates *et al.* (1998), which in turn leads to grain rearrangement and the formation of a new contact network (Fig. 7(b)). The unlocking of the initial fabric creates additional degrees of freedom, leading to a temporary loss of contacts and consequently to the filling of the large voids (void collapse) in a less invasive way when compared to compaction. In fact, densification using mechanical-energy-based methods requires overcoming friction at the contacts, which in some cases may involve abrasion at the contacts and further grain damage and breakage. These phenomena are particularly relevant for carbonate sands, for which the highly angular grains tend to form large voids randomly distributed, as illustrated in Fig. 8 and, in addition, the softness of the grains makes them more prone to damage and breakage.

CONCLUSIONS

This paper explores new mechanisms of thermally induced grain dynamics to enhance sample preparation for laboratory experiments. The experimental observations seem to suggest that the densification of the specimen when submitted to thermal cycling is the result of grain rearrangement due to the additional degrees of freedom created by the expansion of the system. In this way, the density of the sample is increased in a systematic and controllable way without resorting to mechanical energy, which makes this technique less invasive when compared, for example, with compaction techniques. It is shown that sands are more susceptible to densification through thermal cycling when compared with a

Table 3. Coefficient of thermal expansion of materials used in experiments and expected expansion

	Coefficients of linear thermal expansion	Expected expansion
Granular media		
Glass ballotini (soda lime)	9×10^{-6} K^{-1} (Chen *et al.*, 2006)	0·10 μm (0·05% of d_{50})
Calcite ($CaCo_3$)	$6{\cdot}7\times10^{-6}$ K^{-1} (Skinner, 1966)	0·23 μm (0·04% of d_{50})
		0·10 μm (0·04% of d_{50})
Quartz (SiO_2)	$16{\cdot}6\times10^{-6}$ K^{-1} (Skinner, 1966)	0·89 μm (0·10% of d_{50})
Container		
PMMA (acrylic)	77×10^{-6} K^{-1} (ASTM D696 (ASTM, 2008))	148 μm (0·46% of 32 mm container)
Aluminium	$23{\cdot}5\times10^{-6}$ K^{-1} (Hidnert & Krider, 1952)	197 μm (0·14% of 140 mm container)

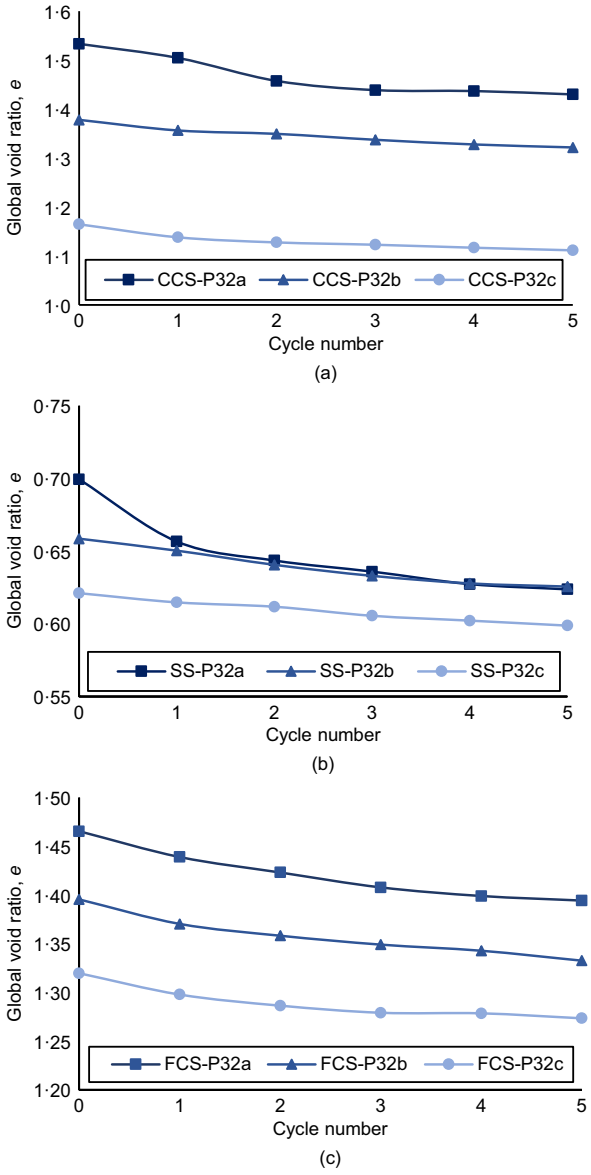

Fig. 6. Void ratio evolution for five thermal cycles using a PMMA container (P32) for: (a) coarse carbonate sand (CCS); (b) silica sand (SS); (c) fine carbonate sand (FCS)

sample of mono-sized spheres, and this is attributed to the complex morphologies and the metastable fabrics found in natural sands. Future work will investigate the additional potential of thermally induced deformation to produce samples with more uniform densities and more stable/mature fabrics.

Table 4. Change in void ratio at end of five thermal cycles for the three sands using the PMMA container

Initial density	ΔD_r (a): % Loose	ΔD_r (b): % Medium dense	ΔD_r (c): % Dense
FCS-P32	8·0	6·9	5·3
CCS-P32	10·3	5·5	5·4
SS-P32	14·4	6·4	4·4

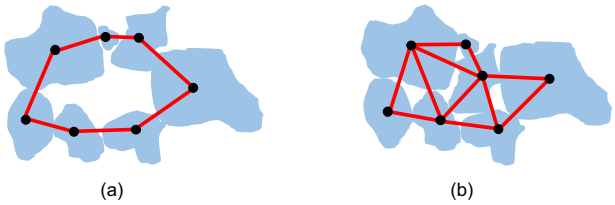

Fig. 7. Schematic diagram illustrating the grain arrangement due to thermal cycling leading to a more compacted fabric (filling of large void) and formation of a new contact network: (a) contact network before thermal cycling; (b) contact network after thermal cycling

Fig. 8. Tomographic image of coarse carbonate sand, taken before thermal cycling, showing the presence of large voids within the material

ACKNOWLEDGEMENT

The authors would like to thank City University London for the doctoral scholarship of the first author.

REFERENCES

ASTM (2008). ASTM D696-08e1: Standard test method for coefficient of linear thermal expansion of plastics between −30°C and 30°C with a vitreous silica dilatometer. West Conshohocken, PA, USA: ASTM International.

ASTM (2016). ASTM D4253-16: Standard test methods for maximum index density and unit weight of soils using a vibratory table. West Conshohocken, PA, USA: ASTM International.

Butterfield, R. & Andrawes, K. Z. (1970). An air activated sand spreader for forming uniform sand beds. *Géotechnique* **20**, No. 1, 97–100, http://dx.doi.org/10.1680/geot.1970.20.1.97.

Camenen, J. F., Cavarretta, I., Hamlin, S. & Ibraim, E. (2013). Experimental and numerical assessment of a cubical sample produced by pluviation. *Géotechnique Lett.* **3**, No. 2, 44–51.

Cates, M. E., Wittmer, J. P., Bouchaud, J. P. & Claudin, P. (1998). Jamming, force chains, and fragile matter. *Phys. Rev. Lett.* **81**, No. 9, 1841.

Cavarretta, I. (2009). *The influence of particle characteristics on the engineering behaviour of granular materials*. PhD thesis, Imperial College London, London, UK.

Chen, K., Cole, J., Conger, C., Draskovic, J., Lohr, M., Klein, K., Scheidemantel, T. & Schiffer, P. (2006). Granular materials: packing grains by thermal cycling. *Nature* **442**, No. 7100, 257.

Cuccovillo, T. & Coop, M. R. (1997). Yielding and pre-failure deformation of structured sands. *Géotechnique* **47**, No. 3, 491–508, http://dx.doi.org/10.1680/geot.1997.47.3.491.

Fonseca, J., O'Sullivan, C., Coop, M. R. & Lee, P.D. (2012). Non-invasive characterisation of particle morphology of natural sands. *Soils Found.* **52**, No. 4, 712–722.

Fonseca, J., O'Sullivan, C., Coop, M. R. & Lee, P. D. (2013). Quantifying the evolution of soil fabric during shearing using scalar parameters. *Géotechnique* **63**, No. 10, 818–829, http://dx.doi.org/10.1680/geot.11.P.150.

Fonseca, J., Reyes-Aldasoro, C. C. & Wils, L. (2015). Three-dimensional quantification of the morphology and intragranular void ratio of a shelly carbonate sand. In *Deformation characteristics of geomaterials: Proceedings of the 6th international symposium on deformation characteristics of geomaterials*, Buenos Aires, Argentina (eds V. A. Rinaldi, M. E. Zeballos and J. J. Clariá), pp. 551–558. Amsterdam, the Netherlands: IOS Press.

Hidnert, P. & Krider, H.S. (1952). Thermal expansion of aluminum and some aluminum alloys. *J. Res. Natn. Bur. Stands* **48**, No. 3, 209–220.

Klotz, E. U. & Coop, M. R. (2001). An investigation of the effect of soil state on the capacity of driven piles in sands. *Géotechnique* **51**, No. 9, 733–751, http://dx.doi.org/10.1680/geot.2001.51.9.733.

Marketos, G. & Bolton, M. D. (2010) Flat boundaries and their effect on sand testing. *Int. J. Numer. Analyt. Methods Geomech.* **34**, No. 8, 821–837.

Miura, S. & Toki, S. (1982). Sample preparation method and its effect on static and cyclic deformation-strength properties of sand. *Soils Found.* **22**, No. 1, 61–77.

O'Donovan, J., Hamlin, S., Marketos, G., O'Sullivan, C., Ibraim, E., Lings, M. & Wood, D. M. (2015). Micromechanics of seismic wave propagation in granular materials. In *Geomechanics from micro to macro* (eds K. Soga, K. Kumar, G. Biscontin and M. Kuo). London, UK: Taylor & Francis Group.

Percier, B., Divoux, T. & Taberlet, N. (2013). Insights on the local dynamics induced by thermal cycling in granular matter. *Europhys. Lett.* **104**, No. 2, 24001.

Rad, N. S. & Tumay, M. T. (1987). Factors affecting sand specimen preparation by raining. *Geotech. Testing J.* **10**, No. 1, 31–37.

Skinner, B. J. (1966). Thermal expansion. In *Handbook of physical constants*, revised edn (ed. S. P. Clark), Memoir 97, pp. 75–96. Boulder, CO, USA: The Geological Society of America, Inc.

Vaid, Y. P. & Negussey, D. (1984). Relative density of pluviated sand samples. *Soils Found.* **24**, No. 2, 101–105.

Wils, L., Van Impe, W. F., Haegeman, W. & Van Impe, P. O. (2013). Laboratory testing issues related to crushable sands. *Proceedings of the 18th international conference on soil mechanics and geotechnical engineering*, Paris, France, pp. 275–278.